Received: 26 April 2021 | Revised: 18 July 2021 | Accepted: 23 July 2021

DOI: 10.1002/ppap.202100063

RESEARCH ARTICLE

PLASMA PROCESSES AND POLYMERS

Cyclic etching of silicon oxide using NF_3/H_2 remote plasma and NH_3 gas flow

You Jung Gill[1] | **Doo San Kim**[1] | **Hong Seong Gil**[1] | **Ki Hyun Kim**[1] | **Yun Jong Jang**[1] | **Ye Eun Kim**[1] | **Geun Young Yeom**[1,2]

[1]School of Advanced Materials Science and Engineering, Sungkyunkwan University, Suwon, Republic of Korea

[2]SKKU Advanced Institute of Nano Technology (SAINT), Sungkyunkwan University, Suwon, Republic of Korea

Correspondence
Geun Young Yeom, School of Advanced Materials Science and Engineering, Sungkyunkwan University, Suwon 16419, Republic of Korea.
Email: gyyeom@skku.edu

Abstract

Selective isotropic cyclic dry etching of silicon oxide (SiO_2) was investigated using a three-step cyclic process composed of hydrogen fluoride (HF) adsorption by NF_3/H_2 remote plasma and reaction with NH_3 gas flow to form ammonium fluorosilicate ($(NH_4)_2SiF_6$), and desorption by heating. The variation of the ratio of NF_3:H_2 (2:1 to 1:3) and adsorption time (10–180 s) showed the highest etch selectivity of SiO_2 over Si_3N_4 at 1:2 ratio of NF_3:H_2 and with the adsorption time of 20 s. The etch selectivity higher than 40 was observed with 20 s of adsorption time with a 1:2 ratio of NF_3:H_2 remote plasma and the total etch depth was linearly increased with the increase of cycles with the SiO_2 EPC of ~7.5 nm/cycle.

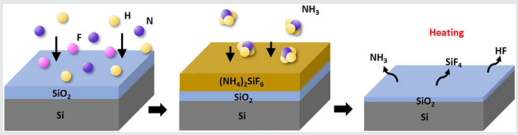

KEYWORDS

cyclic etching, H_2, NF_3, remote plasma, SiO_2

1 | INTRODUCTION

As the device integration is increased and the pattern width is decreased to a few nanometer scale, the requirement of highly selective etching among various materials has been increased further and further for both anisotropic etching and isotropic etching.[1–4] Especially, for isotropic etching, wet etching methods have been generally used to etch materials selectively. However, as the pattern size is decreased to the nanoscale, problems such as pattern sticking due to capillary effect, materials remaining for high aspect ratio patterns due to the difficulty in penetrating the wet solution, wafer damage due to the wet etchant itself, and so forth, become more serious. Therefore, dry isotropic etching is preferred for next-generation semiconductor devices similar to anisotropic etching.[5–8]

Among various isotropic dry etching methods using plasmas, for the selective isotropic etching of oxide over silicon nitride, combinations of F-based gases and H-based reactive gases, such as NF_3/NH_3, OF_2/NH_3, CF_4/NH_3, and so forth, have been investigated with downstream plasmas, remote plasmas, and so forth.[9–11] Downstream or remote-type plasmas have been used not to damage the wafer surface and to increase the etch selectivity by etching radicals only without ion bombardment.[12–15] The combinations of F-based gases and H-based reactive gases are to produce hydrogen fluoride (HF) and to form ammonium fluorosilicate, $(NH_4)_2SiF_6$, through the reaction of silicon oxide with

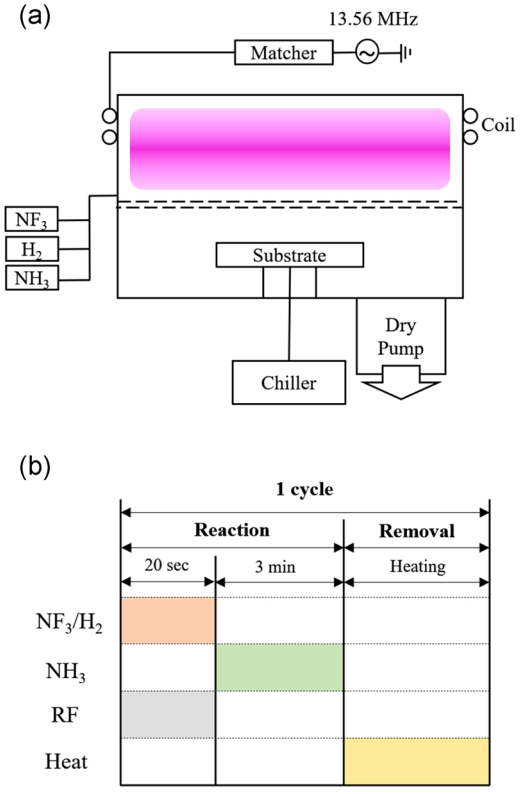

FIGURE 1 (a) Schematic diagram of the remote plasma etching system used in the experiment. (b) Sequence of the cyclic process used for selective and isotropic silicon oxide etching

NH_4F (NH_3 + HF), and where, the ammonium fluorosilicate is vaporized by heating above 100°C.[16–18] During the formation of ammonium fluorosilicate, the thickness of the ammonium fluorosilicate is thicker than that of the consumed silicon oxide due to the compound formation and the thickness of the fluorosilicate is continuously increased with the increase of reaction time. Therefore, it is difficult to control the thickness of reacted oxide and, for the high aspect ratio patterns, if the ammonium fluorosilicate is formed on the sidewall of the patterns, it can be difficult to remove the oxide at the end of the patterns due to the clogging by the ammonium fluorosilicate formed on the sidewall.

These days, for the applications to various semiconductor devices, it is found that it is necessary to control the thickness of etched oxide thickness during the etching in addition to improving high selectivity over silicon nitride. Currently, research of cyclic etch process composed of the formation $(NH_4)_2SiF_6$ on silicon oxide surface by H and F-based plasma followed by NH_3 gas flow and the removal of $(NH_4)_2SiF_6$ through heating has been investigated for selective oxide etch process over silicon nitride but no details are not reported.[9,11,19,20] In this study, we investigated the cyclic etch process of silicon oxide composed of three steps to precisely control the etch amount of silicon oxide and to improve the etch selectivity over silicon nitride, and the

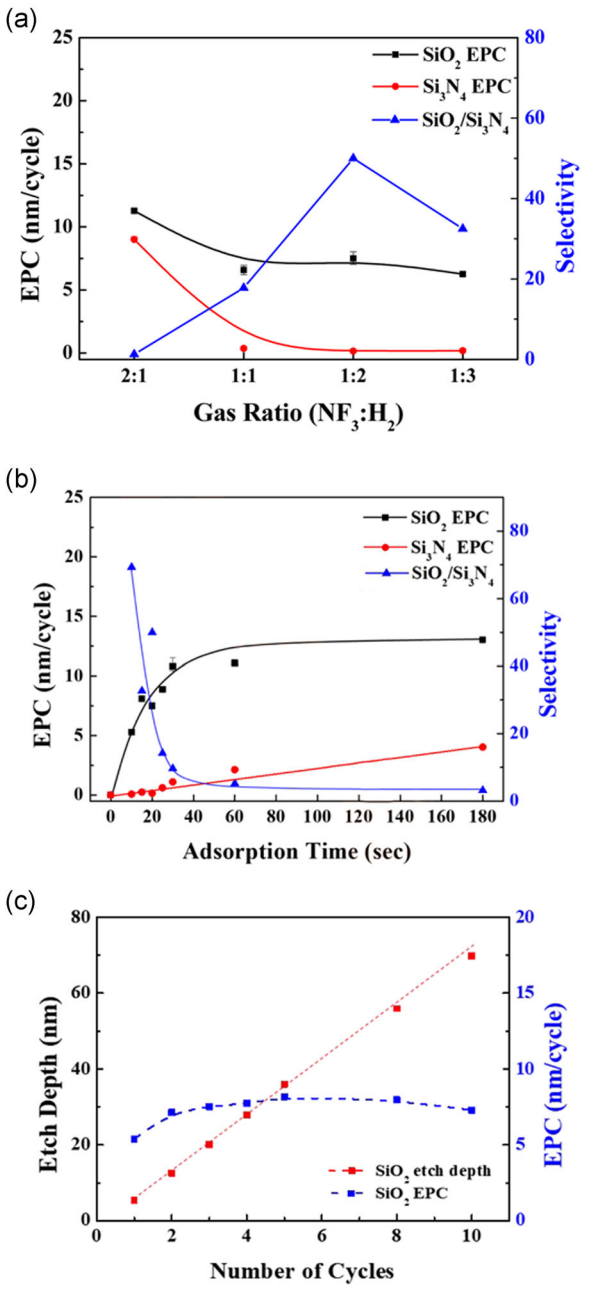

FIGURE 2 (a) EPC and etch selectivity of silicon oxide over silicon nitride measured as a function of NF_3:H_2 gas ratio for 20 s adsorption time. (b) EPC and etch selectivity of silicon oxide over silicon nitride as a function of adsorption time for NF_3:H_2 ratio of 1:2. (c) Etch depth and EPC of silicon oxide measured as a function of the number of etch cycles. EPC, etch depth per cycle

selective etch mechanism has been studied. The three steps are composed of the HF adsorption step by NF_3/H_2 plasma, the reaction step of forming ammonium fluorosilicate by NH_3 flow, and the desorption step by substrate heating. It is found that by using the three-step cyclic process, the silicon oxide etch rate could be precisely controlled as ~7.5 nm/cycle with the etch selectivity over silicon nitride over 40.

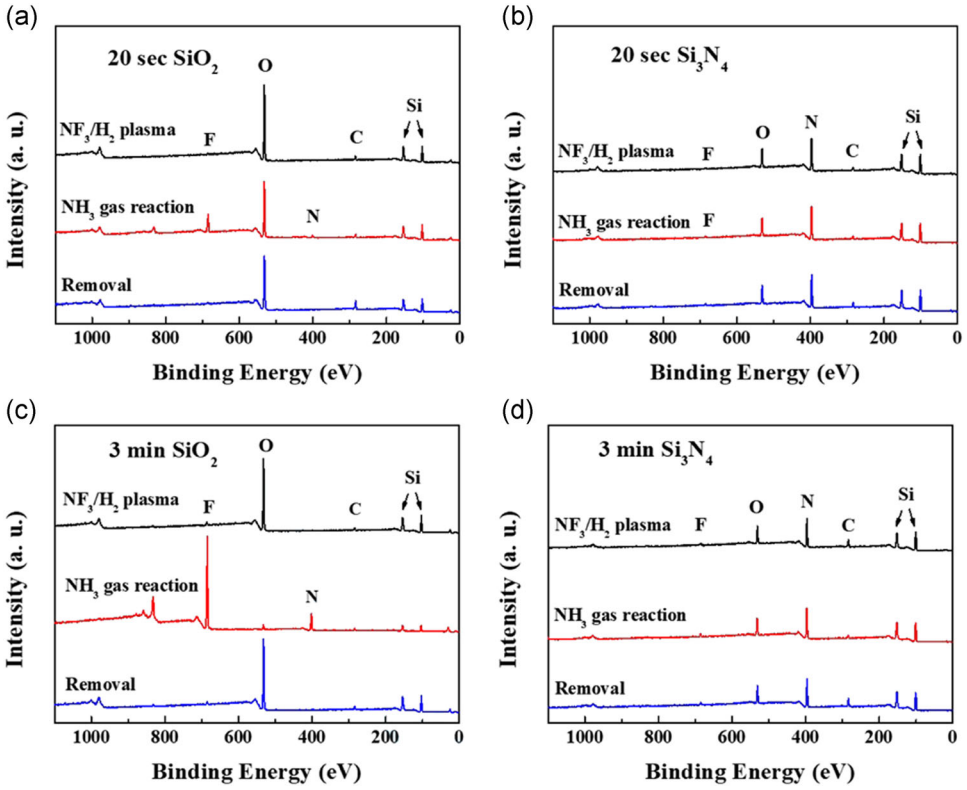

FIGURE 3 XPS wide scan spectra of the surfaces of silicon oxide and silicon nitride after adsorption of 20 s for (a) and (b), and after adsorption of 180 s for (c) and (d), respectively. XPS wide scan spectra were measured after the adsorption, after the reaction with NH_3 for 3 min, and after the desorption by heating at 150°C for 5 min. XPS, X-ray photoelectron spectroscopy

2 | EXPERIMENT

Two hundred-nanometer-thick silicon oxide and 20-nm-thick silicon nitride deposited on silicon wafers by low-pressure chemical vapor deposition (LPCVD) were used to measure the etch depth during the dry etching. In addition, to investigate the etching effect at patterned samples, 15-nm-thick silicon oxide/5-nm-thick silicon nitride deposited by LPCVD to a trench-patterned silicon wafer was also used.

The cyclic dry etching system used in this experiment is shown in Figure 1a. The dry etching source consisted of a remote-type inductively coupled plasma (ICP) with two blocking anodized aluminum grids to confine the plasma in the ICP section and to flow reactive radicals only. A substrate holder was located at the lower part of the chamber and the substrate temperature was controlled by a chiller (JEIO TECH; HTRC-10) and the substrate temperature was measured using a thermocouple in contact with the wafer.

The etching step was composed of three steps as shown in Figure 1b; (1) the adsorption step, where NF_3/H_2 plasma is generated to form and adsorb HF on oxide/nitride surface, (2) the reaction step, where $(NH_4)_2SiF_6$ is formed by NH_3 gas flow, and (3) the desorption step, where the ammonium fluorosilicate is removed by heating. For the adsorption step, the ratio of NF_3:H_2 varied from 2:1 to 1:3 at 200 mTorr and the radical exposure time varied from 10 s ~ 180 s when 300 W 13.56 MHz rf power was applied to the ICP source. For the reaction step, 100 mTorr NH_3 was maintained for 3 min. For the adsorption step and reaction step, the substrate temperature was fixed at 20°C. However, for the desorption step, the substrate was removed from the chamber and heated to 150°C using a hot plate for 5 min to remove the reacted ammonium fluorosilicate.

The etched amounts of silicon oxide and silicon nitride were measured using a spectroscopic ellipsometer (Nano-View SE MG-1000). The surface chemistry during the adsorption step, reaction step, and desorption step was observed by X-ray photoelectron spectroscopy (XPS; ThermoFisher Scientific K-Alpha+). The amount of reaction during the reaction step was observed using Fourier transform-infrared spectroscopy (FTIR; Thermo Electron Nicolet 5700). The depth of radical penetration was measured using secondary ion mass spectrometry (SIMS; IONTOF TOF-SIMS-5). The surface roughness of silicon oxide and silicon nitride during each step was observed using an atomic force microscope (AFM; Park System XE-100). The formation and removal of ammonium

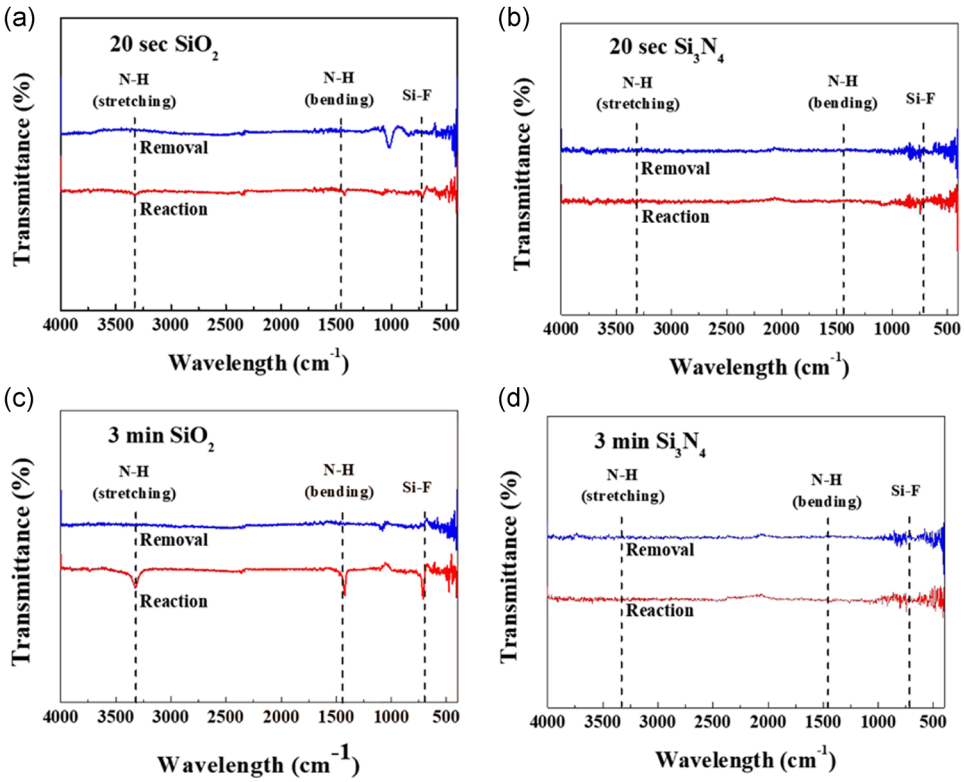

FIGURE 4 FTIR transmission spectra of the silicon oxide and silicon nitride after adsorption of 20 s for (a) and (b), and after adsorption of 180 s for (c) and (d), respectively. FTIR transmission spectra were measured after the adsorption and after the reaction with NH_3 for 3 min. FTIR, Fourier transform-infrared spectroscopy

fluorosilicate formed on patterned samples were observed using a field emission-scanning electron microscope (FE-SEM; HITACHI S-4700).

3 | RESULTS AND DISCUSSION

The effects of process variables of the three-step cyclic process on the etch depth per cycles (EPCs) of silicon oxide and silicon nitrides, and the etch selectivity of silicon oxide over silicon nitrides have been investigated and the results are shown in Figure 2. Figure 2a shows the effect of the ratio of NF_3/H_2 on the EPCs of silicon oxide and silicon nitride and their etch selectivities. The ratio between NF_3:H_2 varied from 2:1 to 1:3 while keeping the operating pressure at 200 mTorr, rf power to ICP source at 300 W, and the adsorption time at 20 s. The substrate temperature was kept at 20°C until the reaction step and the substrate temperature was increased to 150°C during the desorption step using a hot plate. As shown in Figure 2a, the EPCs of both silicon oxide and silicon nitride were decreased with the increase of hydrogen percentage in the NF_3:H_2 mixture; however, the etch selectivity was increased with the increase of H_2 percentage up to 1:2 of NF_3:H_2. At the 1:2 ratio of NF_3:H_2, the etch selectivity of silicon oxide over silicon nitride of over 40 with the silicon oxide EPC of ~7.5 nm/cycle could be obtained. The further increase of H_2 percentage to 1:3 of NF_3:H_2 decreased the etch selectivity possibly due to a more significant decrease in the etched amount of silicon oxide compared to that of silicon nitride.

The effect of radical adsorption time during the three-step cyclic etching on the EPCs and their etch selectivities was investigated and the result is shown in Figure 2b for 1:2 ratio of NF_3:H_2. The radical adsorption time varied from 10 to 180 s at 20°C while maintaining other process conditions as same as those in Figure 2a. As shown in Figure 2b, the initial increase of radical adsorption time from 10 to 20 s during the adsorption step significantly increased the EPC of silicon oxide while it appears to saturate or slowly increase above 20 s. In the case of silicon nitride, the EPC increased slowly than that of silicon oxide and increased almost linearly with the increase of adsorption time. Therefore, the etch selectivity of silicon oxide over silicon nitride initially increased with adsorption time up to 20–60 s but the further increase of adsorption to 180 s decreased the etch selectivity to ~3.2. The change in the etch selectivity with adsorption time during the adsorption step appears to be related to the different diffusion depths of the reactant from the surface to the bulk

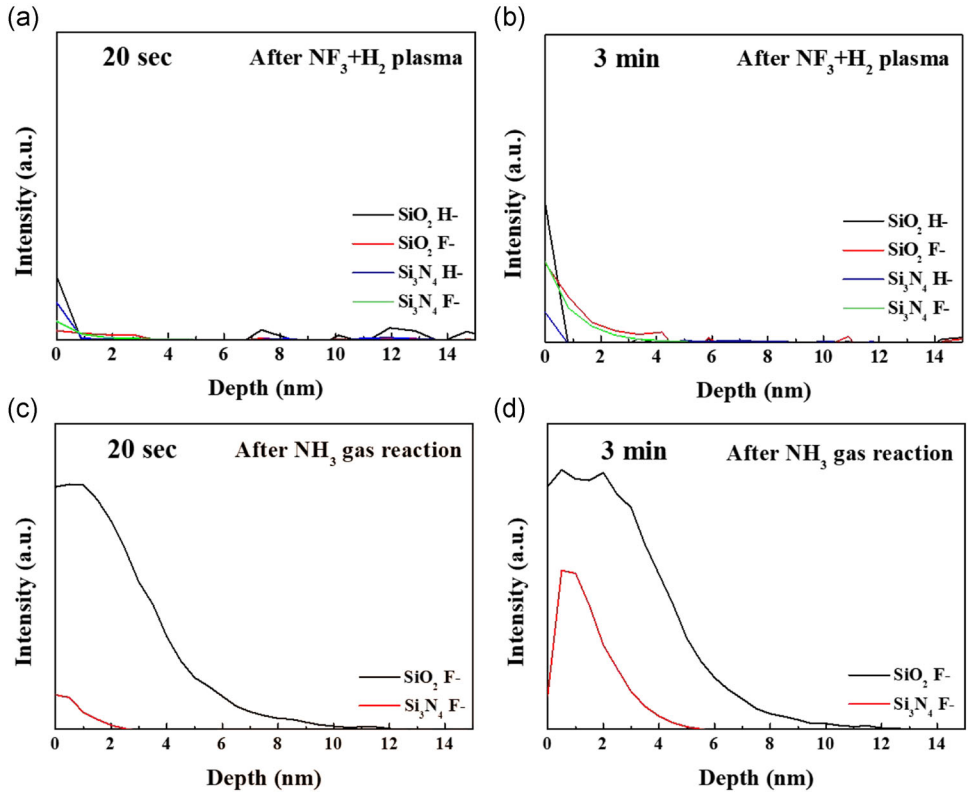

FIGURE 5 SIMS depth profiles of F and H in silicon oxide and silicon nitride after the adsorption with NF_3:H_2 (1:2) plasma for 20 s (a) and 180 s (b). (c) and (d) are SIMS depth profiles of F after the reaction of (a) and (b) with NH_3, respectively. SIMS, secondary ion mass spectrometry

between silicon oxide and silicon nitride. Figure 2c shows the effect of cycles on the etch depth of silicon oxide. As shown in Figure 2c, the etch depth of silicon oxide was almost linearly increased with the increase of etch cycles with the EPC of ~7.5 nm/cycles.

To investigate the reason for the differences in EPCs and etch selectivities at different adsorption times, the surfaces of silicon oxide and silicon nitride after the adsorption with the remote NF_3:H_2 (1:2) plasma for 20 and 180 s, after the reaction with NH_3 for 180 s, and after the desorption were investigated by XPS. The data were measured during the 1st cycle of processing. The results are shown in Figure 3 (a) for the silicon oxide adsorbed for 20 s, (Figure 3b) the silicon nitride adsorbed for 20 s, (Figure 3c) silicon oxide adsorbed for 180 s, and (Figure 3d) silicon nitride adsorbed for 180 s with the NF_3:H_2 (1:2) remote plasma. As shown in Figure 3a,b, for 20 s adsorption, a small F peak was observed after the adsorption on the silicon oxide surface while no noticeable F peak was observed on the silicon nitride surface, and, after the reaction, a bigger F peak intensity was observed for silicon oxide compared to silicon nitride. (The percentages of fluorine after the adsorption, reaction, and removal were 0.94, 13.11, and 1.83% for Figure 3a, and 0.64, 0.94, and 1.52% for Figure 3b.) Similar differences between silicon oxide and silicon nitride were observed for 180 s of adsorption as shown in Figure 3c,d, but much bigger F peak intensities were observed compared to those for 20 s of adsorption. (The percentages of fluorine after the adsorption, reaction, and removal were 2.52, 60.60, and 2.56% for Figure 3c, and 1.75, 2.16, and 2.18% for Figure 3d.) (In the XPS data, the F peak intensity was higher after the reaction compared with that after the adsorption for all cases. In fact, the F peak intensity after the reaction cannot be higher than that after the adsorption because only F remaining after the adsorption step can react with NH_3 and shows the F peak intensity after the reaction. The smaller F peak observed after the adsorption compared with that after the reaction appears to be related to the vaporization of F [or HF] from the surface after the adsorption during the transport for analysis by XPS [it took ~1 day before it was analyzed by XPS after the processing].) The higher F peak intensity observed during the adsorption step is related to the higher F (or HF) diffusion into the surface and the higher F peak intensity observed during the reaction step is related to the thickness of ammonium fluorosilicate formed on the surface by the reaction of F and silicon oxide on the surface with NH_3. Therefore, the F (or HF) content appears to be diffused into the silicon

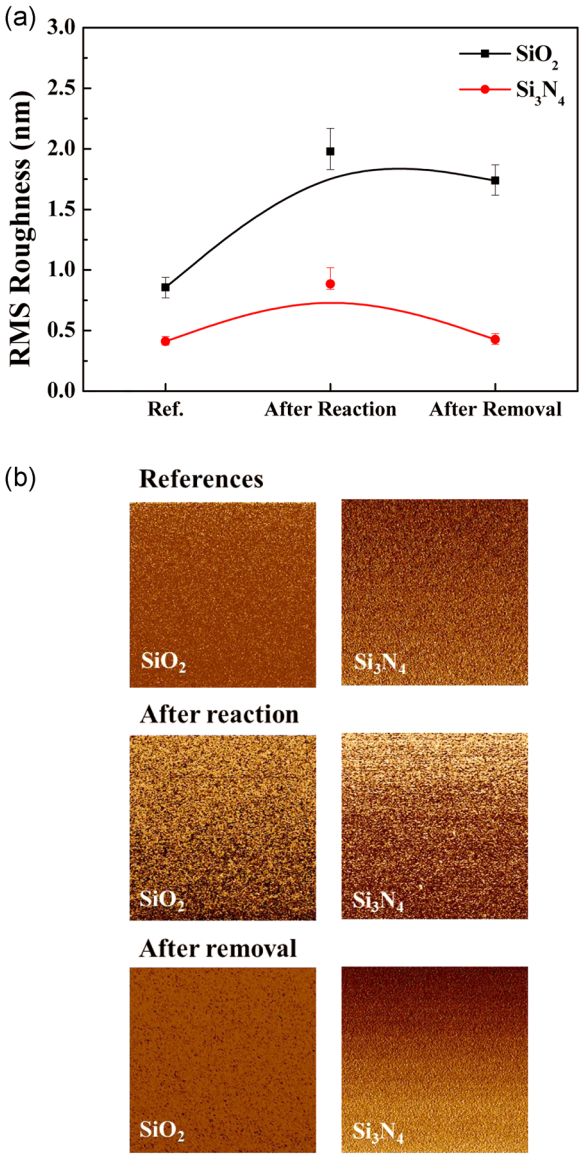

FIGURE 6 RMS surface roughness measured by AFM on the surfaces of silicon oxides and silicon nitrides (adsorbed for 20 s) after the reaction with NH_3 and after the removal of the reacted ammonium fluorosilicate by the heating. (a) RMS surface roughness values measured as a function of the cyclic process step and (b) their surface roughness images. The RMS surface roughness values of the reference silicon oxide and silicon nitride are also shown. AFM, atomic force microscope

oxide more than the silicon nitride and the increase of adsorption time increased the diffused amount of F into the surfaces of both silicon oxide and silicon nitride. The F peak was almost removed on the surfaces of all silicon oxide and silicon nitride after the desorption by the hot plate, indicating the desorption of the ammonium fluorosilicate formed on the surface by heating at 150°C for 5 min.

Figure 4 shows FTIR transmission spectra observed on the surfaces of silicon oxide and silicon nitride reacted with NH_3 after the adsorption for 20 and 180 s with 1:2 of NH_3:H_2. The data were measured during the 1st cycle of processing. The process conditions are the same as those in Figure 3. As shown in Figure 4, no specific absorption peaks could be observed for the silicon nitrides; however, in the case of silicon oxides, peaks related to N–H bending at 1450 cm^{-1}, N–H stretching at 3330 cm^{-1}, and Si–F bonding at 720 cm^{-1} could be observed. Also, the absorption peak intensity was higher for the silicon oxide with the adsorption time of 180 s compared with that of 20 s. Therefore, from the FTIR data, it can be seen that thicker ammonium fluorosilicate is formed on the silicon oxide surface after the adsorption for 180 s compared with that for 20 s and no noticeably thick ammonium fluorosilicate is formed on the silicon nitride surfaces even after the adsorption for 180 s.

SIMS depth profiling has been carried out for the silicon oxides and silicon nitrides shown in Figure 4 and the results are shown in Figure 5. Figure 5a,b show the F and H penetrated into silicon oxide and silicon nitride after the adsorption of 20 and 180 s with the NF_3:H_2(1:2) plasma, respectively, and Figure 5c,d show F penetration after the reaction with NH_3 for 3 min for the samples in Figure 5a,b. The data were measured during the 1st cycle of processing. From the SIMS depth profiles in Figure 5a,b, it can be seen that, for the silicon oxides adsorbed for 20 and 180 s, the depth of penetration of F into silicon oxide estimated by F was measured to ~3.5 and ~4.5 nm after the adsorption for 20 and 180 s, respectively, while that into silicon nitride was measured to be ~1 and ~3 nm for 20 and 180 s, respectively. Hydrogen was not detected in the silicon oxide and silicon nitride. Therefore, the penetration of F was deeper for silicon oxide compared to silicon nitride at the same adsorption time and higher adsorption time increased the depth of penetration. For the samples reacted with NH_3, as shown in Figure 5c,d, the penetration of F was also deeper for the silicon oxide compared with silicon nitride and the penetration depth was increased with increasing adsorption time similar to those adsorbed samples in Figure 5a,b, while the depths of penetration were much deeper than those adsorbed samples. Therefore, similar to XPS data and FTIR data in Figures 3 and 4, it shows that, during the adsorption with the NF_3:H_2 plasma, the diffusion depth of F is smaller for silicon nitride compared to silicon oxide at the same adsorption time and, longer adsorption time (longer than 20 s) not only increases the depth of penetration of F but also decreases the differences in penetration depths between silicon oxide and silicon nitride. Eventually, a thinner ammonium fluosilicate is formed on silicon nitride surfaces compared with silicon oxides, and, the more significant differences in the penetration depth of F between silicon

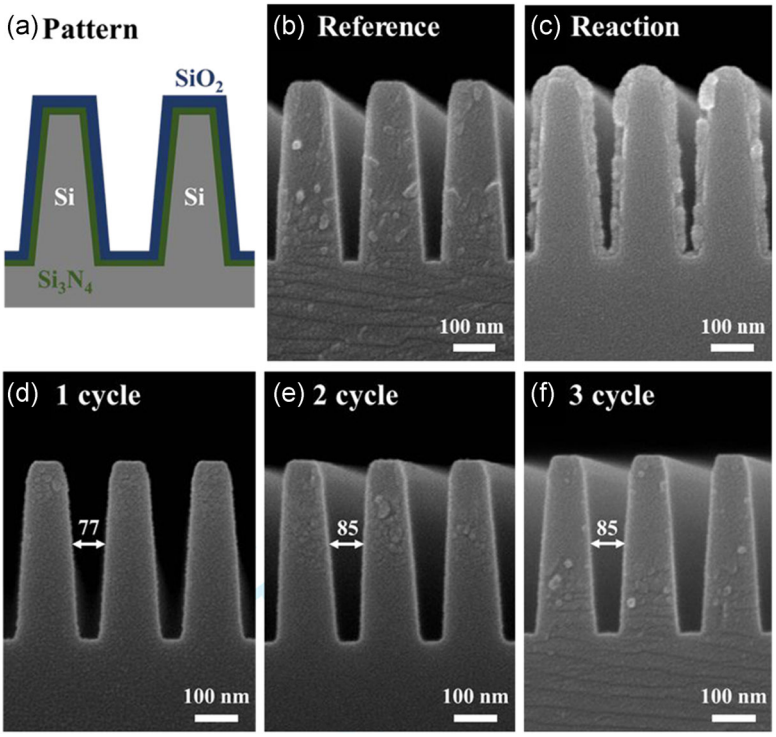

FIGURE 7 SEM images of cyclic etched silicon trenches deposited with ~15 nm thick LPCVD silicon oxide/~5 nm thick silicon nitride; (a) and (b) reference, (c) after the reaction with NH_3 (during 1st cycle), (d) after the desorption of the reacted layer (during 1st cycle), (e) after the desorption of the reacted layer (during 2nd cycle), and (f) after the desorption of the reacted layer (during 3rd cycle). LPCVD, low-pressure chemical vapor deposition; SEM, scanning electron microscope

oxides and silicon nitrides at the adsorption time of 20 s appear to show higher etch selectivity.

Figure 6 shows the RMS surface roughness measured by AFM on the surfaces of silicon oxides and silicon nitrides (adsorbed for 20 s) after the reaction with NH_3 and after the desorption of the reacted ammonium fluorosilicate by the heating. The surface roughness of the as-received (references) silicon oxide and silicon nitride was also measured. As shown in Figure 7, after the reaction, the RMS surface roughness was increased from 0.86 nm to 1.98 nm for silicon oxide and from 0.41 to 0.88 nm for silicon nitride. After the removal of ammonium silicate formed on the silicon oxide and silicon nitride, the surface roughness was decreased to 1.74 nm for silicon oxide and to 0.43 nm for silicon nitride. The increase of surface roughness for both silicon oxide and silicon nitride after the reaction with NH_3 is related to the formation of ammonium fluorosilicate on the surfaces of silicon oxide and silicon nitride; however, even after the removal of the ammonium fluorosilicate, the surface roughness on silicon oxide was increased a little while that on silicon nitride was remaining similar as the reference possibly due to the differences in the thickness of the reacted layer.

Using the adsorption condition of 20 s with the NF_3:H_2 (1:2) plasma in Figure 3, a silicon trench pattern sample covered with 15 nm LPCVD silicon oxide and 5 nm LPCVD silicon nitride was cyclically etched, and the change of trench cross-sectional image was observed. Figure 7a–f shows SEM images of cyclic etched silicon trenches; (Figure 7a,b) reference, (Figure 7c) after the reaction with NH_3 (during 1st cycle), (Figure 7d) after the desorption of the reacted layer (during 1st cycle), (Figure 7e) after the desorption of the reacted layer (during 2nd cycle), and (Figure 7f) after the desorption of the reacted layer (during 3rd cycle). As shown in Figure 7c, after the reaction step, ~20-nm-thick ammonium fluorosilicate appears to be formed uniformly all the trench area and, as shown in Figure 7d, after the desorption step of the 1st cycle, all of the ammonium fluorosilicate appears to be removed and smoother silicon oxide surface is revealed. After the 2nd cycle, the trench width was further increased due to the removal of remaining silicon oxide on the silicon nitride, but, after the 3rd cycle, no changes in trench widths were observed due to the complete removal of silicon oxide on silicon nitride and due to the high etch selectivity of silicon oxide over silicon nitride.

4 | CONCLUSIONS

Using a three-step cyclic process composed of HF adsorption by NF_3/H_2 remote plasma, reaction with NH_3 gas flow, and desorption by heating, the effect of process variables on the EPC of silicon oxide and etch selectivity over silicon nitride was investigated. The change in the NF_3:H_2 ratio showed the highest etch selectivity of silicon oxide over silicon nitride at 1:2 ratio of NF_3:H_2 while decreasing the EPC with the increase of H_2 percentage in the gas mixture. When the NF_3:H_2 plasma exposure time

(adsorption time) was varied, the silicon oxide EPC was nearly saturated at the 20 s after a rapid increase of EPC while the silicon nitride EPC was almost linearly increased with adsorption time; therefore, the highest etch selectivity was observed at the adsorption time of 20 s. XPS, SIMS, and FTIR data showed that, during the NF_3:H_2 plasma exposure, F was diffused significantly deeper into silicon oxide compared to silicon nitride and F was also penetrated deeper for 180 s adsorption time compared with 20 s adsorption time. Therefore, the differences in EPC between silicon oxide and silicon nitride were believed to be related to the diffusion of F (or HF) into the surfaces of silicon oxide and silicon nitride during the NF_3:H_2 plasma exposure. (However, the actual etching can be affected not only by the diffusion of H and F, but also by other factors, such as the compounds formed during this process [NHF, etc.]. In addition, the subsequent reaction with NH_3 gas is also important.) At the optimized condition, the silicon oxide EPC of ~7.5 nm/cycle with the etch selectivity over silicon nitride higher than 40 could be observed with the 20 s of adsorption time and 1:2 ratio of NF_3:H_2 remote plasma. For next-generation 3D devices, various highly selective etching techniques, including selective isotropic dry etching are required; therefore, it is believed that the dry etching technique investigated in this study could be applicable to the fabrication of next-generation 3D semiconductor devices.

ACKNOWLEDGMENTS

This study was supported by the Technology Innovation Program (or Industrial Strategic Technology Development Program—The Development of next-generation intelligent semiconductor technology) (20012609, Atomic Layer Etching Solution and System for Real Time Process Control) funded By the Ministry of Trade, Industry & Energy (MOTIE, Korea) and the MOTIE [Ministry of Trade, Industry & Energy (20003665)] and KSRC (Korea Semiconductor Research Consortium) support program for the development of the future semiconductor device.

REFERENCES

[1] T. Wahlbrink, T. Mollenhauer, Y. M. Georgiev, W. Henschel, J. K. Efavi, H. D. B. Gottlob, M. C. Lemme, H. Kurz, J. Niehusmann, P. Haring Bolivar, *Microelectron. Eng.* **2005**, *78*, 212.
[2] M. Matsui, T. Tatsumi, M. Sekine, *J. Vac. Sci. Technol. A* **2001**, *19*, 1282.
[3] M. Tuda, K. Shintani, J. Tanimura, *Plasma Sources Sci. Technol.* **2003**, *12*, S72.
[4] J. M. Lee, K. M. Chang, H. I. Lee, S. J. Park, *J. Vac. Sci. Technol. B* **2000**, *18*, 1409.
[5] S. J. Pearton, D. P. Norton, *Plasma. Process. Polym.* **2005**, *2*, 16.
[6] H. Puliyalil, U. Cvelbar, *Nanomaterials* **2016**, *6*, 108.
[7] K. F. Shariar, J. Zhang, K. Coasey, M. A. Sufian, R. Remy, J. Qu, M. Mackay, Y. Zeng, *Mater. Res. Express* **2018**, *5*, 095903.
[8] F. Marty, L. Rousseau, B. Saadany, B. Mercier, O. Francais, Y. Mita, T. Bourouina, *Microelectron. J.* **2005**, *36*, 673.
[9] H. J. Oh, J. H. Lee, M. S. Lee, W. G. Shin, S. Y. Kang, G. D. Kim, D. H. Ko, *ECS Trans.* **2014**, *61*, 1.
[10] J. W. Park, M. G. Chae, D. S. Kim, W. O. Lee, H. D. Song, C. H. Choi, G. Y. Yeom, *J. Phys. D Appl. Phys.* **2018**, *51*, 445201.
[11] Y. G. Cho, Y. J. Kim, S. J. Kim, H. Y. Chae, *J. Vac. Sci. Technol. A* **2020**, *38*, 2.
[12] B. E. E. Kastenmeier, P. J. Matsuo, G. S. Oehrlein, J. G. Langan, *J. Vac. Sci. Technol. A* **1998**, *16*, 2047.
[13] E. Pargon, C. P. Etienne, L. Youssef, C. Thomachot, S. David, *J. Vac. Sci. Technol. A* **2019**, *37*, 40601.
[14] J. Li, W. Wang, Y. Li, N. Zhou, G. Wang, Z. Kong, J. Fu, X. Yin, C. Li, X. Wang, H. Yang, X. Ma, J. Han, J. Zhang, Y. Wei, T. Hu, T. Yang, J. Li, H. Yin, H. Zhu, H. H. Radamson, *J. Mater. Sci. Mater. Electron.* **2020**, *31*, 134.
[15] V. Volynets, Y. Barsukov, G. J. Kim, J. E. Jung, S. K. Nam, K. H. Han, S. Huang, M. J. Kushner, *J. Vac. Sci. Technol. A* **2020**, *38*, 023007.
[16] H. Nishino, N. Hayasaka, H. Okano, *J. Appl. Phys.* **1993**, *74*, 1345.
[17] J. Kikuchi, M. Iga, H. Ogawa, S. Fujimura, H. Yano, *Jpn. J. Appl. Phys.* **1994**, *33*, 2207.
[18] K. Shinoda, presented at 19th Int. Conf. on Atomic Layer Deposition, Bellevue, WA, July **2019**.
[19] H. Ogawa, T. Arai, M. Yanagisawa, T. Ichiki, Y. Horiike, *Jpn. J. Appl. Phys.* **2002**, *41*, 5349.
[20] W. S. Kim, W. G. Hwang, I. K. Kim, K. Y. Yun, K. M. Lee, S. K. Chae, *Solid State Phenom.* **2005**, *103–104*, 63.

How to cite this article: Y. J. Gill, D. S. Kim, H. S. Gil, K. H. Kim, Y. J. Jang, Y. E. Kim, G. Y. Yeom. Cyclic etching of silicon oxide using NF_3/H_2 remote plasma and NH3 gas flow *Plasma Processes Polym*. **2021**;18:e2100063.
https://doi.org/10.1002/ppap.202100063